Square and Rectangular Waveguides with Rounded Corners

PAUL LAGASSE AND JEAN VAN BLADEL, SENIOR MEMBER, IEEE

Abstract—**Eigenfunctions, eigenvalues, and attenuation constants in waveguides are determined for the square with rounded corners, and for the cigar-shaped rectangle with rounded ends. These cross sections allow, by continuous variation of a parameter, the investigation of the deformation of the modes and attenuation curves of a circular waveguide. Particular attention is given to the H_{01} mode and its remarkable attenuation curve.**

INTRODUCTION

THE INTERESTING attenuation properties of the H_{01} mode in a circular waveguide have been known for several years [1], [2]. Whereas most waveguide modes have an attenuation that first decreases with frequency, reaches a minimum and thereafter increases monotonically, the H_{01} mode possesses an attenuation that monotonically decreases with increasing frequency. It therefore is tempting to operate the waveguide at very high frequencies in order to achieve low losses. Plans exist to transmit a 50–100-GHz communication band down a copper circular waveguide of 5-cm diameter. In that band the frequency is from 7 to 14 times the cutoff frequency of the H_{01} mode, with the result that hundreds of modes can be propagated. Special precautions are therefore necessary (e.g., the use of mode filters) to avoid propagation of these extraneous power-dissipating modes. Propagation in the H_{01} mode has also been considered for very-high-power transmission. Calculations show that an evacuated copper pipe of 2-m diameter would be able to transmit some 20 GW at 3 GHz without breakdown, at the cost of only 1-dB attenuation per 500 km. It is against this background that we have decided to study the cross sections shown in Fig. 1. In Fig. 1(a), continuous variation of the rounding-off coefficient c/a permits the smooth transition from the circular to the square cross section. In Fig. 1(b), variation of the aspect ratio b/a carries one from a circular to a rectangular cross section with rounded sides. Our analysis has a threefold purpose, as follows.

1) To investigate what happens to the H_{01} mode as the circular shape is distorted, and, in particular, to follow the change that occurs in the attenuation curve. It is expected that the curve will show a particularly flat plateau for some value of c/a or b/a. In the frequency band that corresponds to that plateau, amplitude distortion is low (although phase distortion will still be important).
2) To trace the effects of an imperfection in the circular shape. The first effect is a slight change in the attenuation curve. The second effect is the separation of the cutoff frequencies of the H_{01} and E_{11} modes, which are degenerate for the circular cross section. Degeneracy means that both modes have the same phase velocity. It makes the spillover of energy in the desired H_{01} mode to the undesired E_{11} mode particularly easy. A slight change in the cross section will remove the degeneracy and spread the two cutoff frequencies apart. A typical method for achieving this result is to line the circular waveguide with a thin layer of dielectric. Another method would be to use a slightly elliptical cross section, but this solution is mechanically less desirable. The cross sections of Fig. 1 represent a mechanically acceptable alternative.
3) To facilitate the design of progressive tapers from a rectangular to a circular waveguide [3]. For such a purpose, field structure and cutoff frequency of each intermediate cross section must be known, particularly as broad-banding requires the cutoff frequency to be constant in each cross section. The transition properties of the lowest mode have been investigated previously by means of "superelliptic" cross sections [4]. It is our purpose to give similar data for the transition properties of the higher modes—in particular, the H_{01} mode.

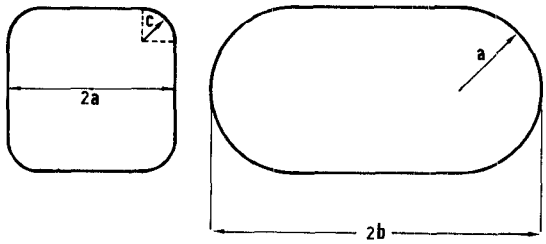

Fig. 1. Cross sections under study.

Manuscript received June 21, 1971; revised August 30, 1971.
The authors are with the Laboratory for Electromagnetism and Acoustics, University of Ghent, Ghent, Belgium.

Formulas for the Mode Losses

A. Derivation of an E Mode

An E mode is derived from a Dirichlet eigenfunction ϕ_m satisfying

$$\nabla^2\phi_m + k_m^2\phi = 0 \tag{1}$$

where $\phi_m = 0$ on the contour C of the cross section S.

With walls having a permeability μ_0 and a high conductivity σ, the fields decrease exponentially according to the law $e^{-\alpha z}$, in which [5]

$$\alpha = \sqrt{\frac{\omega^3\epsilon_0}{8\sigma(\omega^2 - \omega_C^2)}}\,\frac{\int_C \left(\frac{\partial\phi_m}{\partial n}\right)^2 dl}{k_m^2 \iint_S \phi_m^2 dS}. \tag{2}$$

Here ω_C is the cutoff angular frequency $k_m c$ of the mode, and n is the normal to the contour. Let a be a characteristic dimension of the cross section. A universal curve, valid for all E modes in an arbitrary waveguide, can be drawn for αa. The formula, derived from (2), can be written as

$$\alpha a = \sqrt{\frac{(ka)^3}{8k_0 a(k^2a^2 - k_C^2a^2)}}\,M. \tag{3}$$

Here αa is the number of nepers per a, k is the wavenumber, $k_C = k_m$ its value at cutoff, and $k_0 = \sigma\sqrt{\mu_0/\epsilon_0} = \sigma R_0$ is the wavenumber corresponding to the frequency at which $\omega\epsilon_0 = \sigma$. For copper, this frequency is $1.04\ 10^{18}$ Hz, and $k_0 = 2.28\ 10^{10}$ m^{-1}. Factor M is dimensionless and is given by

$$M = \frac{a\int_C \left(\frac{\partial\phi_m}{\partial n}\right)^2 dl}{k_C^2 \iint_S \phi_m^2 dS}. \tag{4}$$

A curve for αa is shown in Fig. 2. The minimum is reached for $k = \sqrt{3}k_c$.

B. Derivation of an H Mode

An H mode is derived from a Neumann eigenfunction ψ_n satisfying

$$\nabla^2\psi_n + k_n^2\psi_n = 0$$
$$\frac{\partial\psi_n}{\partial n} = 0 \text{ on } C. \tag{5}$$

Here, again, universal curves can be drawn starting from the formula [5]

$$\alpha a = \sqrt{\frac{k^2a^2 - k_C^2a^2}{8kak_0a}}\left[P + \frac{k_C^2a^2}{k^2a^2 - k_C^2a^2}Q\right]. \tag{6}$$

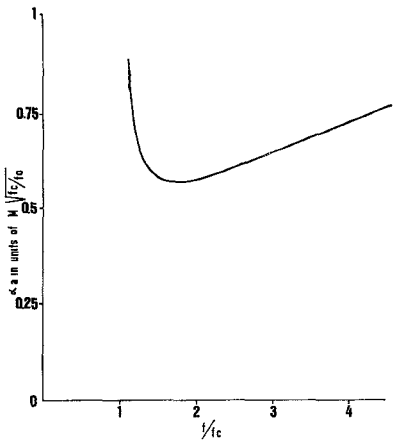

Fig. 2. Universal attenuation curve for the E modes.

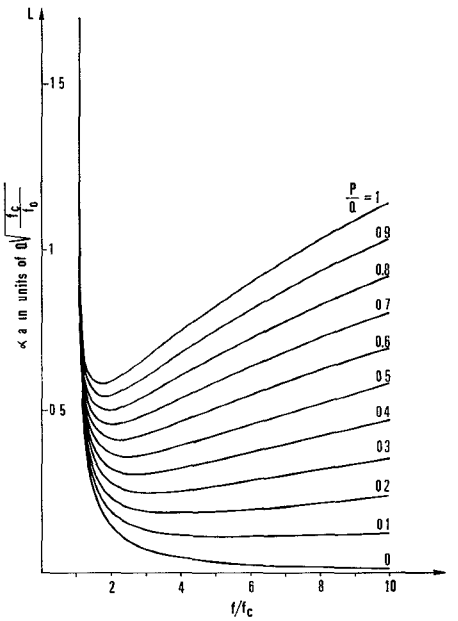

Fig. 3. Universal attenuation curves for the H modes.

In this case there are two dimensionless ratios:

$$P = \frac{a\int_C \left(\frac{\partial\psi_n}{\partial l}\right)^2 dl}{k_C^2 \iint_S \psi_n^2 dS}$$

$$Q = \frac{a\int_C \psi_n^2 dl}{\iint_S \psi_n^2 dS}. \tag{7}$$

Equation (6) shows that the *shape* of the attenuation curves is determined solely by the parameter P/Q. The condition $P = 0$ corresponds to the monotonically decreasing attenuation of mode H_{01}. The value $P/Q = 0.1$

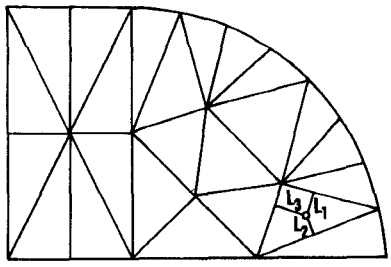

Fig. 4. Relevant to the method of finite elements.

TABLE I

	$k_C a$	P	Q	$\iint \psi^2 dS$
Exact	3.832	0	2	0.5096
Computed	3.845	3×10^{-5}	2.009	0.5081

is about what is needed to obtain a maximally flat curve. Higher values of P/Q give progressively sharper minima (Fig. 3).

The Method of Finite Elements

The functional

$$J(\phi) = \iint_S [|\text{ grad } \phi|^2 - k^2\phi^2]dS \qquad (8)$$

is stationary about the Neumann eigenfunctions of the cross section. With the restriction $\phi = 0$, it becomes stationary about the Dirichlet eigenfunctions. To determine these eigenfunctions, parameter-laden functions are selected according to the principles of the method of finite elements [6], [7]. These functions are introduced in (8), and the parameters are subsequently optimized. Higher order triangular elements were used [8]. Symmetry considerations allowed the computations to be restricted to one quarter of the waveguide cross section. A typical triangular subdivision, as used for the cigar-shaped cross section, is shown in Fig. 4. Within each triangle, the function ϕ is taken to a third-degree polynomial. In the case of Fig. 4 the procedure yields a 133×133 symmetric matrix, the eigenvectors and eigenvalues of which are subsequently computed. The variational parameters are the values of ϕ at certain well-defined points of the triangle. The computation of the different integrals appearing in (4) and (7) has been performed by expressing the third-degree polynomials in terms of the area coordinates L_1, L_2, L_3 indicated in Fig. 4 [6]. In this coordinate system, the various derivatives appearing in the integrals are polynomials in L_1, L_2, L_3, which can easily be evaluated with a computer. The accuracy of the method depends not only on the built-in error of the finite element technique, but also on the error introduced by approximating the circles by straight-line segments. For a rectangular cross section computed with a triangular subdivision of the kind used throughout this paper, the error on the eigenvalues is less than 0.1 percent for the five lowest modes. Using the same triangular net as in the circular part of Fig. 4, results were computed for the H_{01} mode of the circular waveguide and compared with the known exact value (Table I).

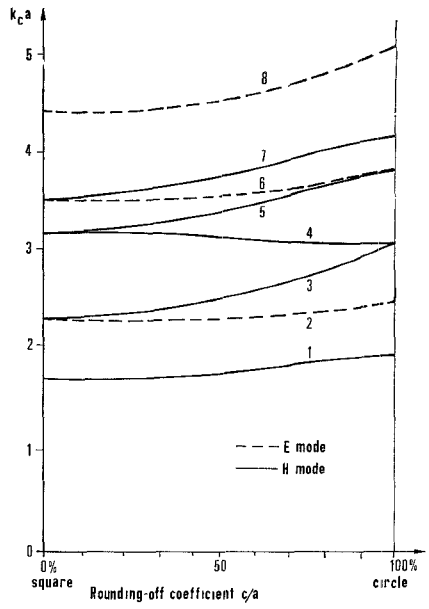

Fig. 5. Cutoff frequency for the square with rounded corners.

As all guides considered in this paper were computed using more elements, and since the curved parts were only a fraction of the complete contour, the errors obtained for the circular guide should give an upper bound to the error of the five lowest modes of the cross sections under study.

The Square–Circle Transition

Computer data for $c/a = 0.3$, 0.5, and 0.7 are presented in Figs. 5 through 10 for some of the lowest modes. Fig. 5 gives the cutoff frequency, or rather the dimensionless parameter $k_C a = 2\pi(a/c)f_C$, as a function of c/a. Notice that the rank of the displayed modes remains unchanged throughout the transition process. Removal of degeneracies through small deformations is evident from the figure. Mode 5 is particularly interesting as it stems from the H_{01} mode in the circular waveguide. The evolution of the curves of constant ψ for this mode is shown in Fig. 6, and similar data appear in Fig. 7 for other modes. The eigenfunction has been normalized to reach a maximum equal to 1. Under each cross section appears the corresponding value of $\iint \phi^2\, dS$ or $\iint \psi^2\, dS$. Although most microwave engineers can imagine how the lines of constant ϕ or ψ are changing from rectangular to square, the plotted curves provide interesting quantitative data. For an E mode the plotted function ϕ is proportional to E_z, and grad ϕ (which can be read off the figure) is proportiona

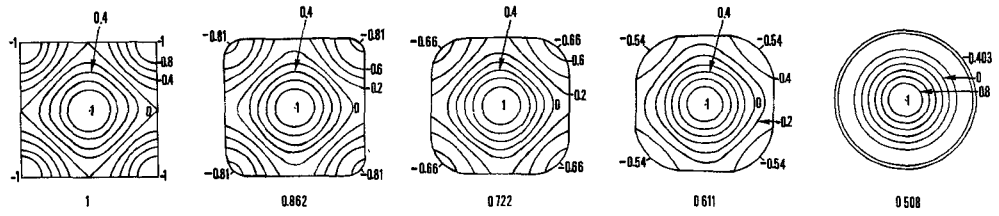

Fig. 6. Lines of constant ψ for mode 5 and $c/a = 1$, 0.7, 0.5, 0.3, and 0.

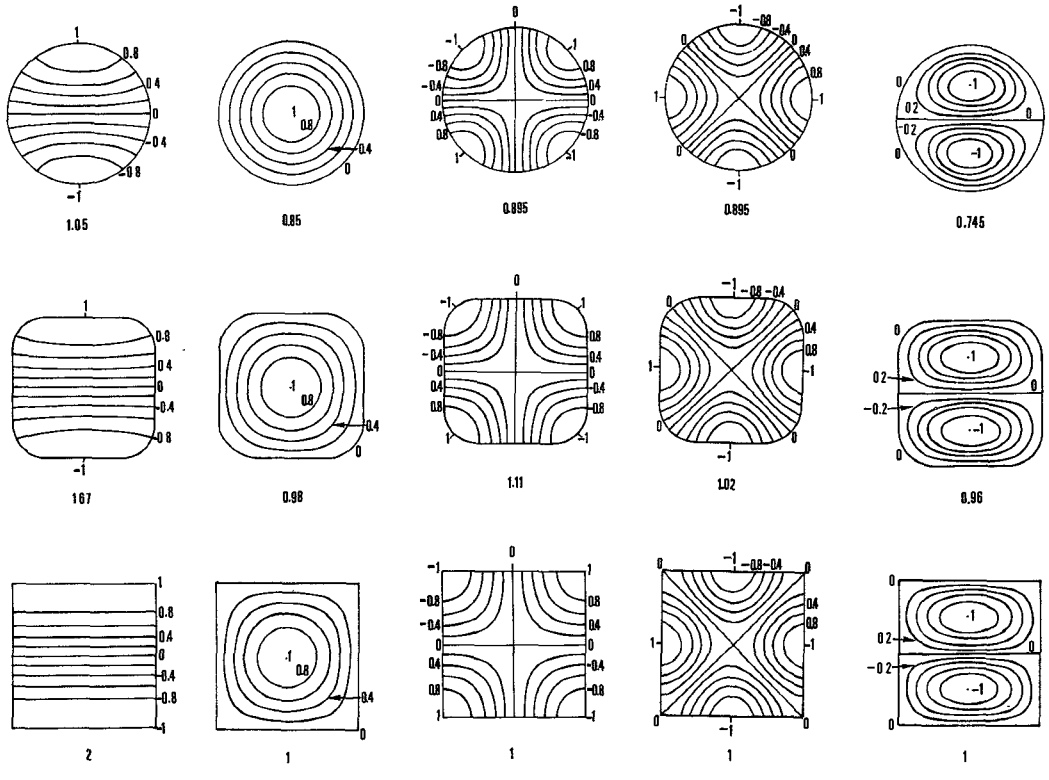

Fig. 7. Lines of constant ϕ or ψ. (a) Mode 1. (b) Mode 2. (c) Mode 3. (d) Mode 4. (e) Mode 6. $c/a = 1$, 0.5, and 0.

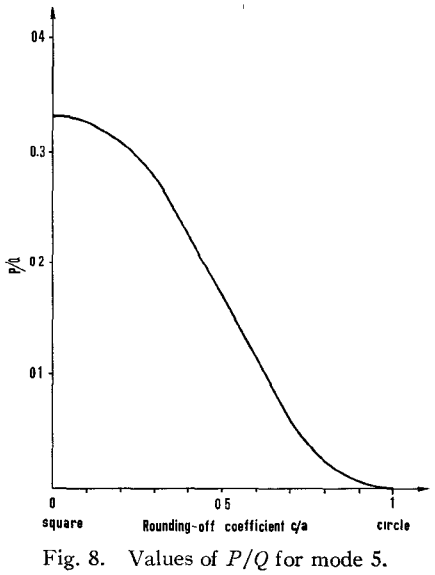

Fig. 8. Values of P/Q for mode 5.

to the transverse electric field $\boldsymbol{E}_{tr}$. The magnetic field $\boldsymbol{H}_{tr}$ is $\boldsymbol{E}_{tr}$ rotated by 90°. For an H mode, the plotted function ψ is H_z, and $\boldsymbol{H}_{tr}$ is grad ψ, while $\boldsymbol{E}_{tr}$ is $\boldsymbol{H}_{tr}$ rotated by 90°. Knowledge of the fields in magnitude and direction allows proper design of launchers and mode filters.

The analytical expressions for the various modes in square and circular waveguides are well known and will not be reproduced here [5]. Explicit calculation of M shows that this parameter has the value 2, and that P/Q stays in the 0–0.5 range for the modes considered. It is found that the values of M and P/Q vary little from square to circle. Nothing drastic will therefore happen with the attenuation curve. The only exception is the fifth mode, where all values of P/Q between 0 1/3 can be obtained by suitable choice of the rounding-off coefficient c/a (Fig. 8). The maximally flat curve is achieved for $P/Q = 0.09$, and corresponds to $c/a = 0.64$.

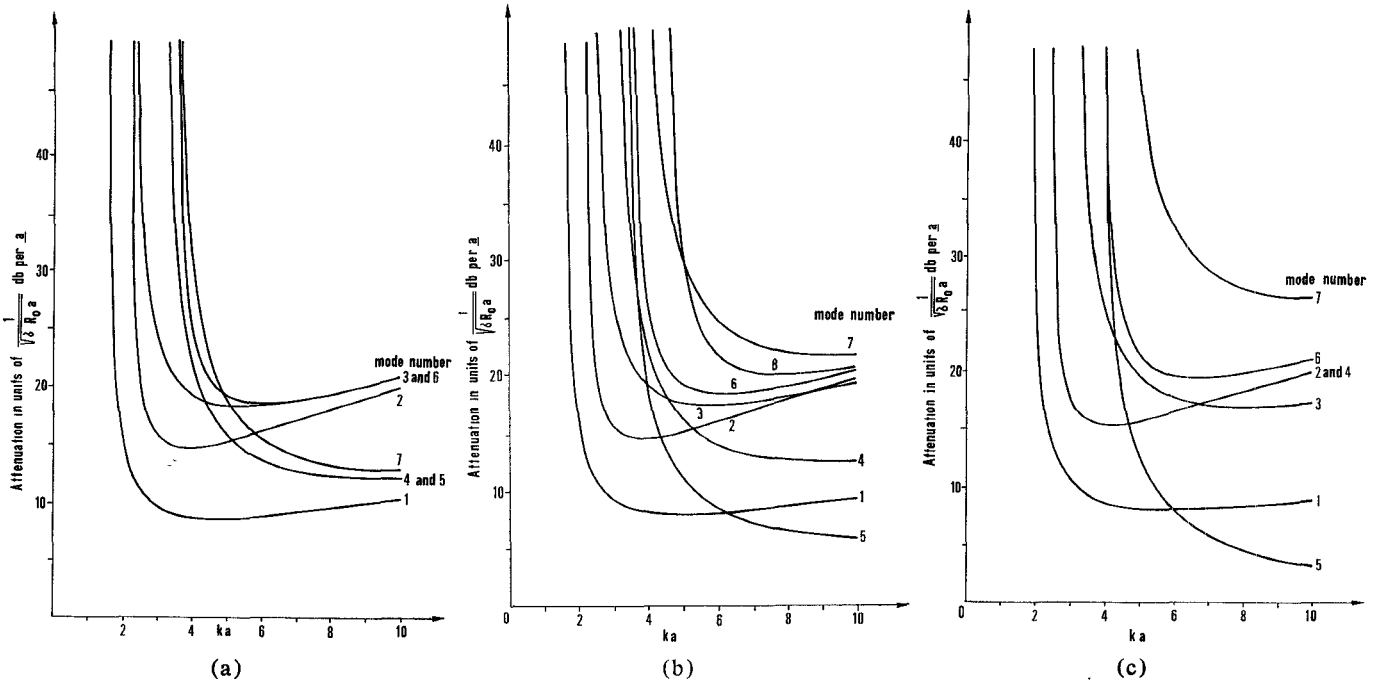

Fig. 9. Attenuation-frequency curves. (a) $c/a=0$ (square). (b) $c/a=0.5$. (c) $c/a=1$ (circle).

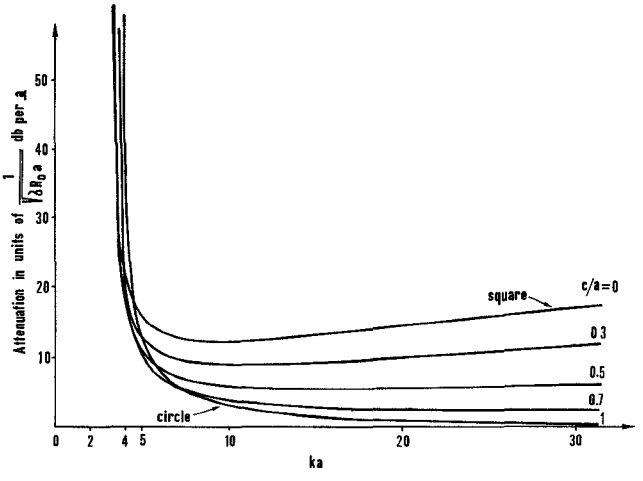

Fig. 10. Attenuation curves for mode 5.

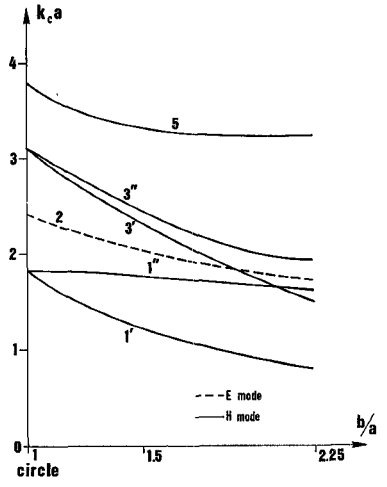

Fig. 11. Cutoff frequency for cigar-shaped cross section.

A few representative attenuation curves are shown in Fig. 9 for the seven lowest modes, and in Fig. 10 for the fifth mode, which, as usual, deserves special attention. The natural unit for the attenuation is the dimensionless parameter $1/\sqrt{\sigma R_0 a}$, where $R_0=377\Omega$. Fig. 10(a) and (c) presents classical results for the attenuation of square and circle. They are included for the sake of comparison with Fig. 10(b), where the effect of the rounded corners has been included.

The Cigar-Shaped Cross Section

Computer data for aspect ratios $b/a=1.5$ and 2.25 are presented in Figs. 11 through 15. The cutoff frequency of the four lowest modes is shown in Fig. 11. These modes have been labeled according to the rank of the circular mode from which they stem. Notice that rank is not conserved. In fact, a picture of more than the four lowest modes becomes hopelessly entangled, as can readily be verified by a glance at the mode chart of a rectangular waveguide. Mode 5, for example, has become the ninth mode for $b/a=1.5$ and the eleventh mode for $b/a=2.25$.

Mode patterns are given in Fig. 12 for the six modes of interest. The transition to the corresponding modes of the rectangular waveguide is displayed. The eigenfunctions of the modes are perhaps apparent from the figure, but here we write them out explicitly for clarity:

$$\cos\frac{\pi x}{a},\quad \cos\frac{\pi y}{2b},\quad \sin\frac{\pi x}{2a}\quad \sin\frac{\pi y}{2b}$$

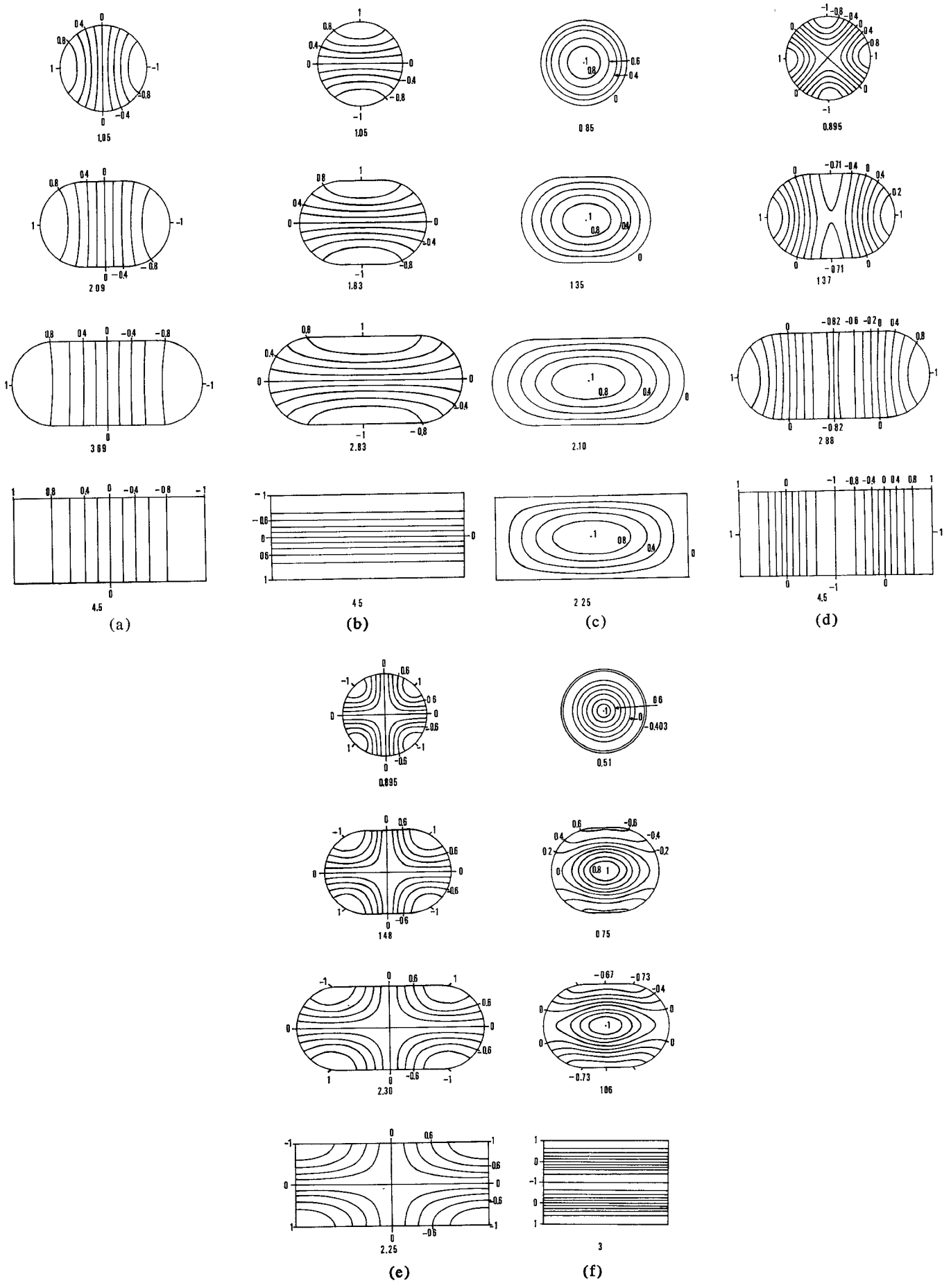

Fig. 12. Lines of constant ϕ or ψ. (a) Mode 1′. (b) Mode 1″. (c) Mode 2. (d) Mode 3′. (e) Mode 3″. $b/a = 1$, 1.5, and 2.25. (f) Mode 5 for $b/a = 1$, 1.25, and 1.5.

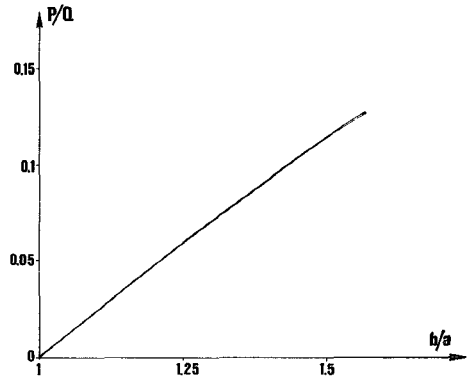

Fig. 13. Values of P/Q for mode 5.

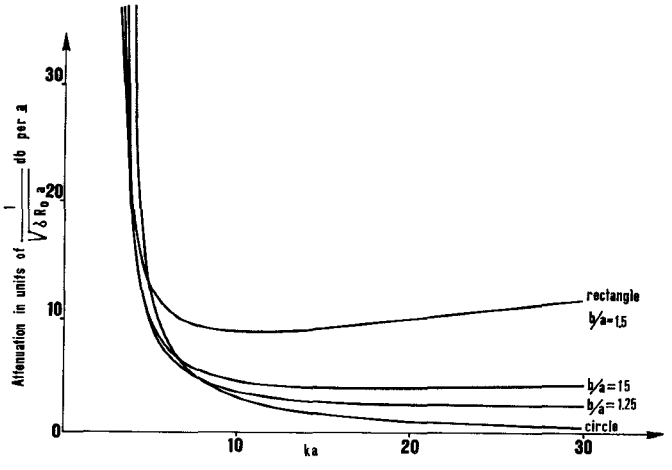

Fig. 14. Attenuation-frequency curve for mode 5.

$$\cos\frac{\pi x}{a},\quad \cos\frac{\pi x}{2a}\quad \cos\frac{\pi y}{2b},\quad \cos\frac{\pi y}{b}$$

respectively, for modes 1′, 1″, 2, 3′, 3″, and 5. Notice that we choose to investigate rather small deformations of the circle for mode 5 ($b/a=1.25$ and 1.5) in order to get a better idea of the influence of mechanical perturbations. Fig. 13 shows the variation of P/Q for this mode, and Fig. 14 some relevant attenuation curves for three values of b/a. Attenuation characteristics of the other modes are shown in Fig. 15.

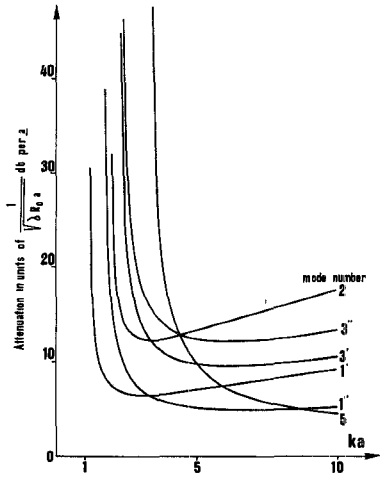

Fig. 15. Attenuation-frequency curves for $b/a=1.5$.

References

[1] A. E. Karbowiak, *Trunk Waveguide Communication*. London, England: Chapman and Hall, 1965.
[2] E. C. Okress, *Microwave Power Engineering*, vol. 1. New York: Academic Press, 1968.
[3] C. C. H. Tang, "On the mode correspondence between circular and square multimode tapered waveguides," *IEEE Trans. Microwave Theory Tech.*, vol. MTT-15, pp. 314–317, May 1967.
[4] T. Larsen, "Superelliptic broadband transition between rectangular and circular waveguides," in *1969 Proc. European Microwave Conf.*, pp. 277–280.
[5] N. Marcuvitz, *Waveguide Handbook*. New York: McGraw-Hill, 1951.
[6] O. C. Zienkiewicz with Y. K. Cheung, *The Finite Element Method in Structural and Continuum Mechanics*. New York: McGraw-Hill, 1968, chs. 10 and 11.
[7] P. Silvester, "Finite element solution of homogeneous waveguide problems," *Alta Freq.*, vol. 38, pp. 313–317, May 1969; also presented at the URSI Symp. Electromagnetic Waves, 1969.
[8] ——, "A general high-order finite-element waveguide analysis program," *IEEE Trans. Microwave Theory Tech.*, vol. MTT-17, pp. 204–210, Apr. 1969.